AIR FORCE REPORT NO.
SAMSO-TR-69-283

AEROSPACE REPORT NO
TR-0066(5306)-3

Some Computational Aspects of the Minimum Fuel Continuous Low Thrust Orbit Transfer Problem

Prepared by J. L. STARR and R. D. SUGAR
Electronics Division

Engineering Science Operations
AEROSPACE CORPORATION

Prepared for SPACE AND MISSILE SYSTEMS ORGANIZATION
AIR FORCE SYSTEMS COMMAND
LOS ANGELES AIR FORCE STATION
Los Angeles, California

Air Force Report No.
SAMSO-TR-69-283

Aerospace Report No.
TR-0066(5306)-3

SOME COMPUTATIONAL ASPECTS OF THE MINIMUM FUEL CONTINUOUS LOW THRUST ORBIT TRANSFER PROBLEM

Prepared by

J. L. Starr and R. D. Sugar
Guidance Analysis Department
Guidance and Navigation Subdivision
Electronics Division

69 AUG 04

Engineering Science Operations
AEROSPACE CORPORATION

Prepared for

SPACE AND MISSILE SYSTEMS ORGANIZATION
AIR FORCE SYSTEMS COMMAND
LOS ANGELES AIR FORCE STATION
Los Angeles, California

FOREWORD

This report is published by the Aerospace Corporation, El Segundo, California, under Air Force Contract Nos. F04701-68-C-0200 and F04701-69-C-0066.

This report, which documents research carried out from May 1968 to March 1969, was submitted for review and approval to 2nd Lt. Edward M. Williams, Jr., SAMSO (SMTAE) on 4 August 1969.

Approved

E. Levin, Director
Guidance and Navigation Subdivision
Electronics Division
Engineering Science Operations

Publication of this report does not constitute Air Force approval of the report's findings or conclusions. It is published only for the exchange and stimulation of ideas.

Edward M. Williams Jr.
Edward M. Williams, Jr.
2nd Lt., USAF
Project Office

ABSTRACT

The purpose of this paper is to examine the computational aspects of the minimum fuel continuous low thrust orbit transfer problem and to display characteristic numerical features introduced by various physical constraints. Minimum-fuel orbit transfer by low thrust is typical of many problems in optimal control which result in a two point boundary value problem which must be solved by some iterative numerical procedure. Two techniques, Multiple Substitution Polynomials (MSP) and Marquardt's method, are shown to be applicable to this task, and a detailed analysis is made of the behavior of these methods in the context of the low thrust problem. A variety of sub-problems is considered with parametric variation of endpoints, thrust-to-weight ratio, and orbit axial orientation. A physical barrier is found which restricts sample points in certain limiting case fixed endpoint transfers. The existence of multiple stationary solutions is shown for the case of intersecting orbits, and the nearly singular behavior in that region is investigated. Numerical results for several transfers are found to compare with similar results reported elsewhere.

CONTENTS

FIGURES

TABLES

GLOSSARY

a	Long's parameter; semimajor axis
e	eccentricity
$\underline{f}(\underline{x}, u)$	system dynamics
G	universal gravitational constant
h	angular momentum
J	cost function
J_a	augmented cost function
M	mass of the earth/satellite system
$\underline{M}$	vector of terminal constraints
MSP	Multiple Substitution Polynomials
m	spacecraft mass
$\dot{m}$	mass flow rate
p	semilatus rectum
R	radius of the earth
r	radial distance from geocenter to spacecraft
s	normalized time
T	thrust magnitude (constant)
TPBVP	two point boundary value problem
T/W	thrust-to-weight ratio
t	time
$\bar{t}$	scaled time
u	scalar control variable

GLOSSARY (Continued)

V	total velocity magnitude
V_ν	circumferential component of velocity
V_r	radial component of velocity
$\underline{x}$	state vector
$\Delta\omega$	axial rotation of the final orbit with respect to the initial orbit
$\jmath$	perturbation parameter
$\underline{\eta}$	constant Lagrange multiplier vector
$\underline{\lambda}(t)$	vector of Lagrange multiplier functions (costate)
μ	gravitational constant for the earth
ν	true anomaly of spacecraft relative to perigee of initial orbit
ϕ	thrust angle measured clockwise from the forward circumferential direction
$\Phi(\underline{x}, t)$	function to be minimized in the Mayer Problem
$(\dot{})$	$\equiv \frac{d}{dt}$ ( )
$(')$	$\equiv \frac{d}{ds}$ ( )

Subscript

0	initial conditions
i	initial orbit
f	final orbit

I. INTRODUCTION

The purpose of this report is to examine computational aspects of the minimum fuel continuous low thrust orbit transfer problem and to display characteristic numerical features introduced by various physical constraints. Computational difficulties in finding numerical solutions of optimal control problems have severely limited the application of modern control theory. The low thrust problem is typical of many optimal control problems for which the necessary conditions may be established, and yet which defy analytic solution (without drastic simplification) or straightforward numerical solution because of computational difficulties.

Orbit transfer by low thrust has received considerable attention in the past decade (Refs. 1 - 5), and numerical solutions have been obtained for a large variety of subproblems in the control of low-thrust vehicles. However, in emphasizing the physical characteristics of the problem, the computational complexities have been somewhat overlooked. There has been little mention of the behavior of various numerical techniques, or of a comparison of techniques. Very often the schemes employed have been severely limited in general application, and, in most cases, the extreme sensitivity of the solution to the choice of initial conditions has dictated knowing the form of the solution a priori. The two point boundary value problem (TPBVP) arising from the low thrust problem has been solved by Newton-Raphson techniques (Refs. 2, 5), quasilinearization (Ref. 3), and dynamic programming (Ref. 6), although the computational difficulties encountered have usually been formidable for all but the simplest of orbit transfer conditions, for example, circle-to-circle coplanar transfers.

In this report, numerical solutions are obtained for ellipse-to-ellipse transfers, with several combinations of fixed and free endpoints. Of particular interest is the minimum fuel transfer between given elliptical orbits in which both endpoints are free. Optimal solutions are obtained numerically for transfers between rotated coplanar elliptical orbits, and the existence of multiple extrema is demonstrated. Two finite dimensional optimization techniques,

Multiple Substitution Polynomials (MSP) and Marquardt's method, will be examined in the context of the low thrust orbit transfer problem. Attention will be focused on obtaining a successful iterative convergent process with emphasis on the numerical algorithm, the method of reduction of the problem for computational purposes, and the behavior of neighboring solutions for parametric studies.

The problem to be considered is (refer to Fig. 1) to determine the optimal thrust orientation history to transfer a constant magnitude, low-thrust vehicle by having it thrust continuously from an initial orbit to some desired terminal orbit, with the minimum expenditure of fuel. The initial and terminal orbits are assumed to lie in a common plane about a spherical, drag-free earth. Thus, the only forces acting on the vehicle are its thrust and its own weight. Plane polar coordinates are chosen for the geometry of the problem, with the thrust orientation angle measured clockwise from the circumferential direction. The assumption of a constant mass flow rate transforms the minimum fuel problem to a minimum time problem, with fuel expenditure linearly proportional to total transfer time.

The orbits chosen have perigee/apogee altitude values of 55/110 and 80/180 n mi. Initially, the orbits are taken as co-apsidal ($\Delta\omega = 0$ deg), but results are obtained for various axial rotations. A thrust-to-weight ratio of $T/W = 0.0125$ is initially assumed; the effects of varying T/W are also investigated.

The nature of the physical problem itself and the structure of the resulting TPBVP have led to a set of three Cases which are described in Table 1. Reference will be made extensively throughout the rest of the paper to Cases I, II, and III. Case I consists of transfers between fixed points on the initial and terminal orbits whose locations are specified in advance. The solution of the TPBVP yields the optimum thrust orientation history as well as the transfer trajectory and fuel expenditure. Case II consists of transfers from a specified point on the initial orbit to a point (not specified in advance) on the terminal orbit, the location of which is an additional part of the problem. Case III consists of fuel optimal transfers between orbits in which neither the departure nor arrival point is fixed in advance, but must be determined as part of the solution to the problem.

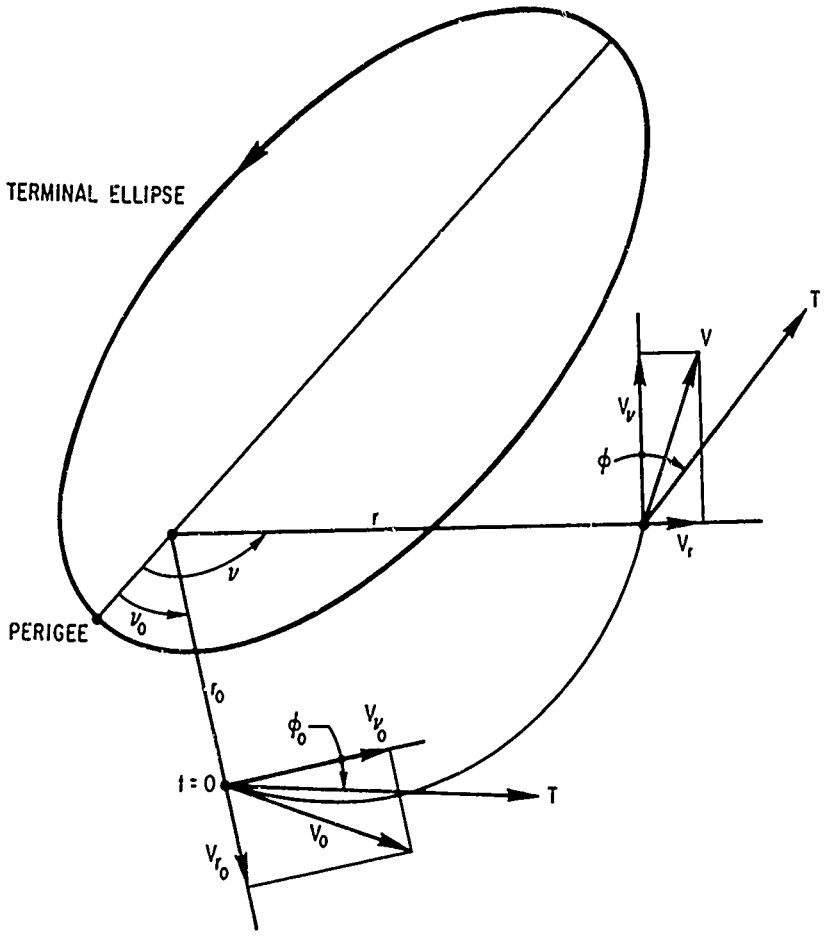

NOTATION

e_f = terminal ellipse eccentricity

h_f = terminal ellipse angular momentum

m = spacecraft mass

$\dot{m}$ = mass rate (constant)

p_f = terminal ellipse semilatus rectum

r = radial distance to spacecraft

T = thrust magnitude (constant)

t_f = final time

t = time

V_ν = circumferential component of velocity

V_r = radial component of velocity

V = total velocity $V = \left(V_r^2 + V_\nu^2\right)^{1/2}$

μ = gravitational constant

ν = angular position of spacecraft relative to perigee of terminal orbit

ϕ = thrust angle

subscript 0 refers to initial conditions

Figure 1. Geometry and Nomenclature of the Orbit Transfer

Table 1. Orbit Transfer Cases

Case	Physical Interpretation	TPBVP Interpretation
I	Fuel optimal transfer from a fixed point in the initial orbit to a fixed point in the terminal orbit	Fixed endpoint optimization problem
II	Fuel optimal transfer from a fixed point in the initial orbit to a point (not fixed) in the terminal orbit	One endpoint fixed, one endpoint free optimization problem
III	Fuel optimal transfer between two orbits in which neither departure nor arrival point is fixed in advance	Two free endpoints optimization problem

II. FORMULATION OF THE PROBLEM

A. DYNAMIC EQUATIONS AND SPECIFIED BOUNDARY CONDITIONS

Using the notation defined in Fig. 1, the equations of motion for the non-atmospheric spherical earth gravitational model are:

$$\dot{r} = V_r$$

$$\dot{\nu} = \frac{V_\nu}{r}$$

$$\dot{V}_r = \frac{V_\nu^2}{r} - \frac{\mu}{r^2} + \frac{T \sin \phi}{(m_0 - |\dot{m}|t)}$$

$$\dot{V}_\nu = - \frac{V_r V_\nu}{r} + \frac{T \cos \phi}{(m_0 - |\dot{m}|t)} \qquad (1)$$

The initial conditions are specified by:

$$r(t_0) = \frac{p_i}{1 + e_i \cos \nu(t_0)}$$

$$\nu(t_0) = \nu_{0spec} \qquad \text{(Cases I and II only)}$$

$$V_r(t_0) = \frac{e_i h_i \sin \nu(t_0)}{p_i}$$

$$V_\nu(t_0) = \frac{h_i}{r(t_0)} \qquad (2)$$

with the terminal conditions given as

$$r(t_f) = \frac{p_f}{1 + e_f \cos \nu(t_f)}$$

$$\nu(t_f) = \nu_{fspec} \qquad \text{(Case I only)}$$

$$V_r(t_f) = \frac{e_f h_f \sin \nu(t_f)}{p_f}$$

$$V_\nu(t_f) = \frac{h_f}{r(t_f)} \tag{3}$$

where the subscripts i and f refer to the initial and final orbits; e_i, a_i, e_f, and a_f are specified orbital parameters (eccentricity and semimajor axis); and h_i, p_i, h_f, p_f are the corresponding angular momentum and semilatus rectum for each ellipse.

The orbit transfer is to be made by orienting the thrust vector at the best instantaneous angle $\phi(t)$, measured clockwise from the circumferential direction, to minimize the total fuel expenditure for the maneuver. Since a constant mass flow rate is assumed, a minimum time transfer is equivalent to minimizing the fuel. This can be viewed as a classical Mayer Problem in the Calculus of Variations, and the necessary conditions for optimality are reviewed in the next section.

B. NECESSARY CONDITIONS FOR OPTIMALITY: THE MAYER PROBLEM

It is desired to minimize the criteria function of the form

$$J = \Phi(\underline{x}, t)\Big|_{t=t_f} \tag{4}$$

subject to the differential equation constraints

$$\dot{\underline{x}} = \underline{f}(\underline{x}, u) \quad , \quad \underline{x}_0 = \underline{x}(t_0) \tag{5}$$

where $\underline{x}$ and $\underline{f}$ are n-vectors and u is a scalar function of time, and to the specified terminal constraints.

$$\underline{M}(\underline{x}, t)\big|_{t=t_f} = \underline{0} \tag{6}$$

where $\underline{M}$ is an m-vector with $m \leq n$. If, for example, the complete state vector is specified at the terminal point (as in the Case I orbital transfer), then

$$M_1 = r_f - \frac{p_f}{1 + e_f \cos \nu_{fspec}}$$

$$M_2 = \nu_f - \nu_{fspec}$$

$$M_3 = V_{r_f} - \frac{e_f h_f \sin \nu_{fspec}}{p_f}$$

$$M_4 = V_{\nu_f} - \frac{h_f}{r_f} \tag{7}$$

Consider further the free time problem where the final time t_f is not specified The augmented cost function is constructed as

$$J_a = \Phi(\underline{x}_f, t_f) + \underline{\eta}^T \underline{M}(\underline{x}_f, t_f) + \int_{t_0}^{t_f} \underline{\lambda}^T(t)[\dot{\underline{x}} - \underline{f}(\underline{x}, u)]dt \tag{8}$$

where $\underline{\lambda}(t)$ is an n-vector of Lagrange multiplier functions and $\underline{\eta}$ is a constant m-vector of Lagrange multipliers.

Requiring that the first variation of J_a vanish yields the Euler-Lagrange equations

$$\dot{\underline{\lambda}}^T = -\underline{\lambda}^T \frac{\partial \underline{f}(\underline{x}, u)}{\partial \underline{x}} \qquad \text{[costate equations]} \quad (9)$$

and

$$\underline{\lambda}^T \frac{\partial \underline{f}(\underline{x}, u)}{\partial u} = 0 \qquad \text{[optimality condition]} \quad (10)$$

and boundary conditions

$$\underline{\lambda}^T(t_f) = \frac{\partial \Phi}{\partial \underline{x}} + \underline{\eta}^T \frac{\partial \underline{M}}{\partial \underline{x}} \qquad \text{[transversality conditions]} \quad (11)$$

$$(\underline{\lambda}^T \dot{\underline{x}})\Big|_{t_f} = -\frac{\partial \Phi}{\partial t} - \underline{\eta}^T \frac{\partial \underline{M}}{\partial t} \quad (12)$$

In principle, Eq. (10) may be solved at each time point for the instantaneous control

$$u = u(\underline{x}, \underline{\lambda}) \quad (13)$$

and substitution may be made into Eq. (9) to give the reduced adjoint equation

$$\dot{\underline{\lambda}} = \underline{g}(\underline{x}, \underline{\lambda}) \quad (14)$$

where

$$\underline{g}(\underline{x}, \underline{\lambda}) = -\left[\frac{\partial \underline{f}(\underline{x}, u(\underline{x}, \underline{\lambda}))}{\partial \underline{x}}\right]^T \underline{\lambda}$$

If an iterative numerical procedure is required to calculate u(t), starting estimates must be made in a region where $\underline{\lambda}^T \partial^2 \underline{f}/\partial u^2 < 0$, as required by the Weierstrass Condition. An analytic solution must satisfy this condition as well.

The boundary conditions for Eq. (14) are given at the final time by Eq. (11), whereas the initial conditions of the state equations, Eq. (5), are known. Hence, the original optimization problem of Mayer has been transformed into a two-point boundary value problem (TPBVP). If Eq. (5) is a set of non-linear dynamic equations, an analytic solution of the TPBVP is not possible except under extremely unusual circumstances. To sum up, the unknown quantities are:

		no. of elements
$\underline{\lambda}_0 \equiv \underline{\lambda}(t_0)$		n
$\underline{\eta}$		m
t_f		1
	Total	n + m + 1 unknowns

The conditions to be satisfied are:

			no. of elements
$\underline{M}$	terminal constraints	Eq. (6)	m
$\underline{\lambda}(t_f)$	transversality	Eq. (11)	n
$(\underline{\lambda}^T \dot{\underline{x}})\|_{t_f}$		Eq. (12)	1
		Total	m + n + 1 conditions

Thus it is seen n + m + 1 unknowns are available to satisfy an equal number of conditions; the system is determined.

C. REDUCTION OF THE TRANSVERSALITY CONDITIONS

Since the minimum fuel orbit transfer using a continuous-burning constant mass flow rate engine requires a minimum time traversal, the

appropriate Mayer problem cost function is $\Phi(x(t), t)\big|_{t_f} = t_f$.

The state variables may be assigned as:

$$x_1 = r$$

$$x_2 = \nu$$

$$x_3 = V_r$$

$$x_4 = V_\nu \tag{15}$$

The specified terminal conditions (Eq. 6) for Case I become

$$M_1 = x_{1f} - \frac{p_f}{1 + e_f \cos x_{2f}}$$

$$M_2 = x_{2f} - \nu_{fspec}$$

$$M_3 = x_{3f} - \frac{e_f h_f \sin x_{2f}}{p_f}$$

$$M_4 = x_{4f} - \frac{h_f}{x_{1f}} \tag{16}$$

Thus

$$\frac{\partial \underline{M}}{\partial \underline{x}} = \begin{bmatrix} 1 & -\dfrac{p_f e_f \sin x_{2f}}{\left(1 + e_f \cos x_{2f}\right)^2} & 0 & 0 \\ 0 & 1 & 0 & 0 \\ 0 & -\dfrac{e_f h_f \cos x_{2f}}{p_f} & 1 & 0 \\ \dfrac{h_f}{x_{1f}^2} & 0 & 0 & 1 \end{bmatrix} \tag{17}$$

and since $\partial\Phi/\partial\underline{x} = (0, 0, 0, 0)$, Eq. (11) gives

$$\begin{aligned} \lambda_{1f} &= \eta_1 - \frac{p_f e_f \sin x_{2f}}{\left(1 + e_f \cos x_{2f}\right)^2} \eta_2 \\ \lambda_{2f} &= \eta_2 \\ \lambda_{3f} &= -\frac{e_f h_f \cos x_{2f}}{p_f} \eta_2 + \eta_3 \\ \lambda_{4f} &= \frac{h_f}{x_{1f}^2} \eta_1 + \eta_4 \end{aligned} \tag{18}$$

The Lagrange multipliers η_1, η_2, η_3, η_4 have no specified values and thus the λ_{1f}, λ_{2f}, λ_{3f}, λ_{4f} are undetermined for the Case I boundary conditions.

For Case II transfers, the specified boundary conditions are

$$M_1 = x_{1f} - \frac{p_f}{1 + e_f \cos x_{2f}}$$

$$M_2 = x_{3f} - \frac{e_f h_f \sin x_{2f}}{p_f}$$

$$M_3 = x_{4f} - \frac{h_f}{x_{1f}} \tag{19}$$

Thus

$$\begin{bmatrix} \frac{\partial M_1}{\partial x_1} & \frac{\partial M_1}{\partial x_2} & \frac{\partial M_1}{\partial x_3} & \frac{\partial M_1}{\partial x_4} \\ \frac{\partial M_2}{\partial x_1} & \frac{\partial M_2}{\partial x_2} & \frac{\partial M_2}{\partial x_3} & \frac{\partial M_2}{\partial x_4} \\ \frac{\partial M_3}{\partial x_1} & \frac{\partial M_3}{\partial x_2} & \frac{\partial M_3}{\partial x_3} & \frac{\partial M_3}{\partial x_4} \end{bmatrix} = \begin{bmatrix} 1 & -\frac{p_f e_f \sin x_{2f}}{\left(1 + e_f \cos x_{2f}\right)^2} & 0 & 0 \\ 0 & -\frac{e_f h_f \cos x_{2f}}{p_f} & 1 & 0 \\ \frac{h_f}{x_{1f}^2} & 0 & 0 & 1 \end{bmatrix} \tag{20}$$

Then since $\Phi_{\underline{x}} = (0, 0, 0, 0)$,

$$\left.\begin{aligned} \lambda_{1f} &= \eta_1 + \frac{h_f}{x_{1f}^2}\eta_3 \\ \lambda_{2f} &= -\frac{p_f e_f \sin x_{2f}}{\left(1 + e_f \cos x_{2f}\right)^2}\eta_1 - \frac{e_f h_f \cos x_{2f}}{p_f}\eta_2 \\ \lambda_{3f} &= \eta_2 \\ \lambda_{4f} &= \eta_3 \end{aligned}\right\} \text{Transversality conditions in terms of Lagrange multipliers } \underline{\eta} \tag{21}$$

Thus, the terminal coupling of the state and adjoint variables can be expressed as

$$\lambda_{2f} + \frac{p_f e_f \sin x_{2f}}{\left(1 + e_f \cos x_{2f}\right)^2}\left(\lambda_{1f} - \frac{h_f}{x_{1f}^2}\lambda_{4f}\right) + \frac{e_f h_f \cos x_{2f}}{p_f}\lambda_{3f} = 0 \qquad (22)$$

If the transfer is constrained to depart from the initial ellipse, but at an unspecified exit point, an additional set of transversality conditions arises leading to

$$\lambda_{20} + \frac{p_i e_i \sin x_{20}}{\left(1 + e_i \cos x_{20}\right)^2}\left(\lambda_{10} - \frac{h_i}{x_{10}^2}\lambda_{40}\right) + \frac{e_i h_i \cos x_{20}}{p_i}\lambda_{30} = 0 \qquad (23)$$

Thus Eq. (22) and (23) serve to couple both the initial and final state and costate variables, and, although the unknowns ν_0 and ν_f cannot be determined directly from these, they provide the additional information necessary to establish the optimal values.

D. SCALING OF THE VARIABLES

The state variables are scaled into characteristic units in the following manner:

(a) Time: $$\bar{t} = (\mu/R^3)^{1/2} t = Ct \qquad (24)$$

where

t = unscaled time, in seconds
μ = GM
R = radius of the earth
G = universal gravitational constant
M = mass of the earth/satellite system;

the scaling constant C has radians/second as the units and is the mean angular velocity of a surface circular satellite.

(b) Length: $\bar{r} = r/R$ (25)

where r = radial distance to satellite measured from the center of the earth, in feet.

(c) Velocity: $\bar{V} = V/RC$ (26)

where V = velocity of satellite in feet/second and the product $RC = (\mu/R)^{1/2}$ and is thus the velocity of a surface circular satellite measured in feet/second.

(d) Time normalization (Long's transformation):

For computational purposes, it is convenient to introduce a new independent variable s by the transformation

$$\bar{t} = as \tag{27}$$

where $0 \leq s \leq 1$ and a is a constant.

Thus when s = 1, $a = \bar{t}_f$ (the scaled final time). Integration is performed with respect to s for a fixed number of steps, since its range is constrained to the unit interval. For free (variable) time problems, the value of the unknown parameter a is determined as part of the optimization process. The variable s is referred to as "normalized time." From Eqs. (24) and (27), the differential relationship is seen to be

$$dt = \frac{a}{c}\, ds \tag{28}$$

and the state and costate differential equations are transformed accordingly.

Corresponding to the scaled state dynamic equations is the adjoint system

$$\lambda_1' = \frac{\bar{V}_\nu \lambda_2}{\bar{r}^2 R} + \frac{\bar{V}_\nu^2 C\lambda_3}{\bar{r}^2} - \frac{2C\lambda_3}{\bar{r}^3} - \frac{\bar{V}_r \bar{V}_\nu C\lambda_4}{\bar{r}^2}$$

$$\lambda_2' = 0$$

$$\lambda_3' = -\frac{\lambda_1}{C} + \frac{\bar{V}_\nu \lambda_4}{\bar{r}}$$

$$\lambda_4' = -\frac{\lambda_2}{RC\bar{r}} - \frac{2\bar{V}_\nu \lambda_3}{\bar{r}} + \frac{\bar{V}_r \lambda_4}{\bar{r}} \qquad (29)$$

where $(\,)' \equiv d(\,)/ds$. The adjoint variables can thus be nondimensionalized by selecting the following scaling relations

$$\bar{\lambda}_1 = \lambda_1$$

$$\bar{\lambda}_2 = \lambda_2/R$$

$$\bar{\lambda}_3 = C\lambda_3$$

$$\bar{\lambda}_4 = C\lambda_4 \qquad (30)$$

E. REDUCTION TO STANDARD FORM FOR COMPUTATION

The necessary conditions which must be satisfied by the optimal orbital transfer trajectory constitute a nonlinear two point boundary value problem which in general does not admit an analytic solution. The unknown parameters which must be determined to solve the TPBVP are the initial condition vector for the costate differential system $\underline{\lambda}_0$ and the free (unspecified) final transfer time t_f. These must be adjusted to satisfy the transversality conditions at the initial and final point, when applicable, and the specified elements of the terminal state vector.

For computational purposes, it is convenient to define a vector function $\underline{\Gamma}$ in the following manner:

$$\underline{\Gamma} = \begin{bmatrix} \underline{M} \\ \hline \underline{T} \end{bmatrix} = \begin{bmatrix} M_1 \\ \vdots \\ M_m \\ \hline T_1 \\ \vdots \\ T_{n-m+1} \end{bmatrix} \tag{31}$$

where $\underline{M}$ represents the specified conditions on the state vector and $\underline{T}$ consists of the transversality conditions (in reduced form). Thus since the functions in $\underline{\Gamma}$ are evaluated at times t_f and t_0 (for Case III),

$$\begin{aligned} \underline{\Gamma} &= \underline{\Gamma}(\underline{x}_0, \underline{\lambda}_0, \underline{x}_f, \underline{\lambda}_f, t_f) \\ &= \underline{\Gamma}[\underline{x}_0, \underline{\lambda}_0, \underline{x}_f(\underline{x}_0, \underline{\lambda}_0, t_f), \underline{\lambda}_f(\underline{x}_0, \underline{\lambda}_0, t_f), t_f] \\ &= \underline{\Gamma}(x_i(t_0), \underline{\lambda}_0, t_f) \end{aligned} \tag{32}$$

where $x_i(t_0)$ designates the unspecified elements of $\underline{x}_0 = \underline{x}(t_0)$. A vector of unknowns is next defined as

$$\underline{y} = \begin{bmatrix} \underline{\lambda}_0 \\ \hline x_i(t_0) \\ \hline t_f \end{bmatrix} \tag{33}$$

and hence the problem is transformed into the following:
find $\underline{y}^*$ such that

$$\underline{\Gamma}(\underline{y}^*) = \underline{0} \tag{34}$$

where $\underline{0}$ is the zero vector of proper dimension and $\underline{y}^*$ is the optimal value of $\underline{y}$; or in the equivalent scalar form, find

$$\min_{\underline{y}} ||\underline{\Gamma}(\underline{y})||$$

where it is known from the definition of $\underline{\Gamma}$ that the minimum norm is zero.

The simplicity of the relation Eq. (34) is deceptive in that the solution $\underline{y}^*$ may be extremely difficult to obtain. There are several reasons for this: (1) since $\underline{y}$ represents initial conditions on differential equations, the value of the function $\underline{\Gamma}$ is very sensitive to small changes in its argument; (2) $\underline{\Gamma}$ can be evaluated only after integration of the state and costate differential equations from t_0 to t_f, which involves many computations and numerical integration errors that may become critical here; (3) the contours of $||\Gamma||$ are almost always highly irregular and contain narrow channels and multiple extrema. Nevertheless, the above problem may, in principle, be solved by numerical techniques which are applicable for multivariable function minimization.

III. DESCRIPTION OF THE ALGORITHMS

Two finite dimensional optimization techniques which were employed for solving the nonlinear boundary value problems for the optimal orbit transfer are reviewed in this section. The basic principles of the algorithms will be discussed briefly. For further details the reader should consult the references.

A. MULTIPLE SUBSTITUTION POLYNOMIALS

This is an iterative gradient-free optimization technique which acts to generate a sequence of substitute contour systems for the vector function $\underline{\Gamma}(\underline{y})$. Each of these in turn is treated by standard techniques applicable for solving simultaneous nonlinear algebraic equations. R. F. Jaggers (Ref. 7) has developed the following method for calculating and applying multivariable substitution polynomials in dynamic optimization problems.

The basic plan is to represent the vector function $\underline{\Gamma}(\underline{y})$ by a system of second-order multivariable polynomials as follows:

$$\begin{aligned}
\Gamma_1(y_1, \ldots, y_n) &= \sum_{i=0}^{n}\sum_{j=i}^{n} a_{ij}^{(1)} y_i y_j \\
\Gamma_2(y_1, \ldots, y_n) &= \sum_{i=0}^{n}\sum_{j=i}^{n} a_{ij}^{(2)} y_i y_j \\
&\;\;\vdots \qquad\qquad \vdots \qquad\qquad \vdots \\
\Gamma_n(y_1, \ldots, y_n) &= \sum_{i=0}^{n}\sum_{j=i}^{n} a_{ij}^{(n)} y_i y_j
\end{aligned} \tag{35}$$

where $\underline{y} = (y_1, \ldots, y_n)^T$ is the vector of unknowns and the $a_{ij}^{(k)}$ are constant coefficients to be determined. By definition, $y_0 = 1$ so both constant and

first order terms are also present in the representation. It is convenient to define a transformation

$$z_i = (y_i - E_i)/\Delta_i \qquad i = \ldots, n \tag{36}$$

where E_i represents the best estimate of y_i^* and the Δ_i are selected scaling parameters. Thus Eq. (35) becomes

$$\Gamma_1 = \sum_{i=0}^{n}\sum_{j=i}^{n} A_{ij}^{(1)} z_i z_j$$

$$\Gamma_2 = \sum_{i=0}^{n}\sum_{j=i}^{n} A_{ij}^{(2)} z_i z_j$$

$$\vdots \qquad \vdots \qquad \vdots$$

$$\Gamma_n = \sum_{i=0}^{n}\sum_{j=i}^{n} A_{ij}^{(n)} z_i z_j \tag{37}$$

where the constants $A_{ij}^{(k)}$ are related to the $a_{ij}^{(k)}$, but only the former need to be determined. These coefficients may be calculated without recourse to a matrix inversion, using the algorithm developed by Jaggers. See Ref. 7 or 8 for details of this procedure.

The next step is to set the right side of Eq. (37) to the zero vector and find the vector $\underline{z} = (z_1, \ldots, z_n)^T$ which satisfies $\underline{\Gamma}(\underline{z}) = \underline{0}$. Denoting by $\underline{z}^{(k)} = (z_1^{(k)} \ldots, z_n^{(k)})^T$ the solution of the k^{th} substitute contour system (i.e., the k^{th} iteration), the corresponding value for $\underline{y}^{(k)}$ is

$$y_i^{(k)} = \Delta_i z_i^{(k)} + E_i \qquad i = 1, \ldots, n \tag{38}$$

It is not presumed that this $\underline{y}^{(k)}$ is the exact solution to the original problem since it can be only as precise as the approximation used in Eq. (37). Instead, $\underline{y}^{(k)}$ is treated as the new best estimate of the true optimum $\underline{y}^{*}$ and, accordingly, $E_i = y_i^{(k)}$ is substituted. New polynomial representations are generated, centered about this new estimate, and the procedure continues as before. Iterations are continued until $\underline{\Gamma}(\underline{y}^{(k)}) \to \underline{0}$ to the required tolerance. The procedure is schematically illustrated in Fig. 2 where an approximation for a single function of two variables is given. The solution of the substitute contour system after the i^{th} iteration (denoted by $\underline{E}^{(i+1)}$) can be found, for example, by using the Newton-Raphson algorithm. The gradient which is required can readily be calculated analytically from the quadratic form as follows:

$$\frac{\partial \Gamma_\ell}{\partial z_k} = A_{0k} + \sum_{j=1}^{n} \alpha_{kj} A_{kj}^{(\ell)} z_j \qquad \begin{matrix} k = 1, \ldots, n \\ \ell = 1, \ldots, n \end{matrix} \tag{39}$$

where

$$\alpha_{kj} = \begin{cases} 2 \text{ if } k = j \\ 1 \text{ if } k \neq j \end{cases}$$

and

$$A_{kj}^{(\ell)} = A_{jk}^{(\ell)} \qquad \text{if} \qquad k > j$$

The polynomials are established by evaluating actual function $\underline{\Gamma}$ at test points of the form

$$y_i = \begin{cases} E_i + \Delta_i \\ E_i \\ E_i - \Delta_i \end{cases} \qquad i = 1, \ldots, n \tag{40}$$

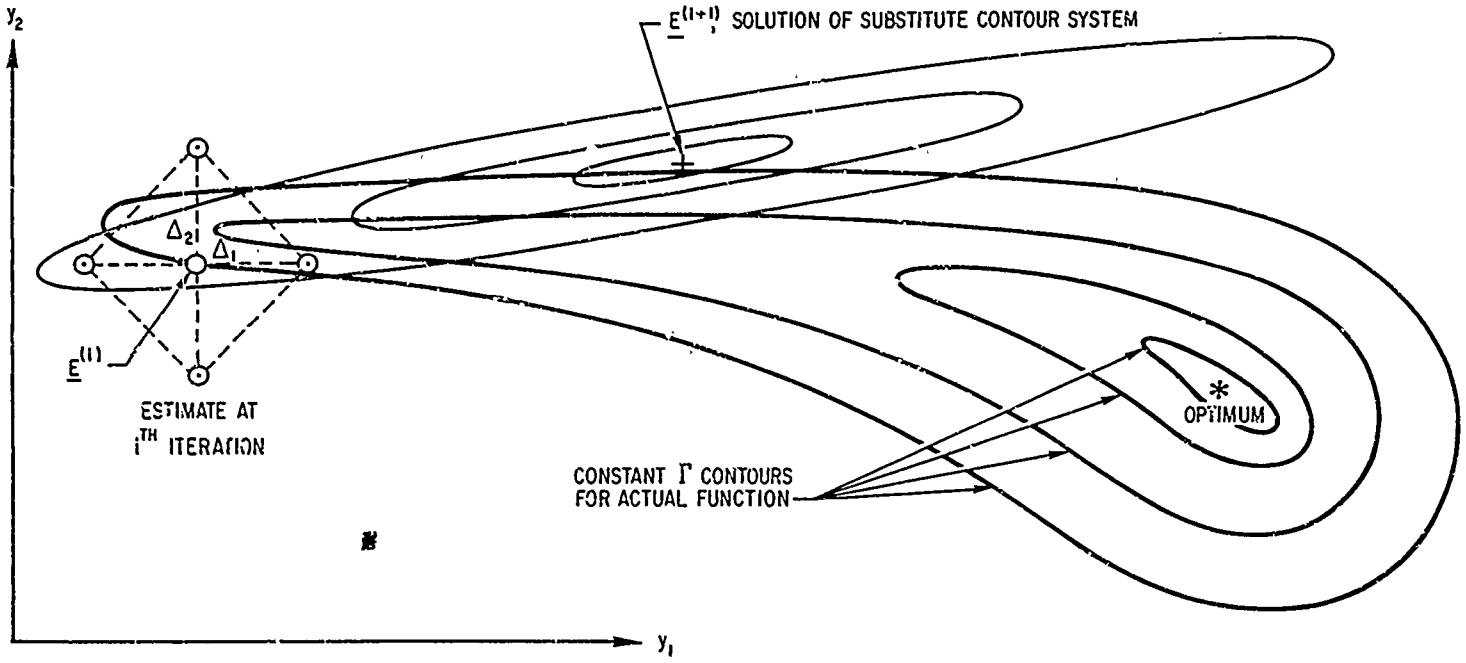

$$\Gamma = \Gamma(y_1, y_2) \approx \sum_{i=0}^{2} \sum_{j=i}^{2} a_{ij} y_i y_j, \quad y_0 = 1$$

Figure 2. Multiple Substitution Polynomials Method: Heuristic View

and the representation is made via multivariable interpolation formulas which agree with the actual function at these test points only. The scale parameters Δ_i should be selected relatively large when beginning the iterations and reduced under program control, as the solution is approached, to refine the region of interest. The desired situation occurs when the test points "straddle" the solution, i.e., have most of the Γ_i change sign when the $+\Delta_i$ and $-\Delta_i$ test points are used. Convergence on subsequent iterations will then usually proceed quite rapidly.

The principal features of the multiple substitution polynomial method are: (1) the gradient of the function $\underline{\Gamma}$ is not required; (2) the general n dimensional algorithm allows easy computer application, and programming effort and computer storage requirements are minimal; and (3) convergence is rapid in the neighborhood of the solution. This technique was found to perform well for parametric studies of the fixed endpoint orbit transfer problem.

The computational difficulties which arise in applying MSP are related to the accuracy of the contour approximation and the iterative solution of the substitute contour system. When the approximation is relatively weak, a minimum norm solution of the latter can sometimes be used effectively when the zero norm does not exist. An efficient iterative method for solving the generated simultaneous nonlinear algebraic equations is essential for success since loss of convergence here causes a breakdown of the whole procedure. The Newton-Raphson algorithm with an automatic convergence monitor was found to give good results.

B. MARQUARDT'S ALGORITHM

This is a gradient-oriented method which seeks to combine the principal features of the Taylor series method (i.e., Newton-Raphson) and the gradient method (steepest descent) by performing an adaptive interpolation between them. The basic idea is to solve the desired system $\underline{\Gamma}(\underline{y}^*) = \underline{0}$ by generating a correction vector $\underline{\Delta y}^{(i)} = \underline{y}^{(i+1)} - \underline{y}^{(i)}$ which minimizes the scalar function

$$S(\underline{\Delta y}) = (\underline{\Gamma}(\underline{y}) + A\underline{\Delta y})^T(\underline{\Gamma}(\underline{y}) + A\underline{\Delta y}) + \lambda(\underline{\Delta y}^T\underline{\Delta y} - R^2) \tag{41}$$

where $A = \partial\underline{\Gamma}/\partial\underline{y}$ is the gradient matrix evaluated at the point $\underline{y}$, and λ is a scalar Lagrange multiplier associated with a correction size constraint $\underline{\Delta y}^T\underline{\Delta y} = R^2$. R is a positive constant representing the radius of a hypersphere over which the minimization of S is to be performed. The appropriate minimizing correction vector corresponding to Eq. (41) is readily shown to be

$$\underline{\Delta y} = - (A^T A + \lambda I)^{-1} A^T \underline{\Gamma}(\underline{y}) \tag{42}$$

It is of interest to observe that the correction step given by the Newton-Raphson algorithm is

$$\underline{\Delta y}_{NR} = - A^{-1} \underline{\Gamma}(\underline{y}) \tag{43}$$

which corresponds to the limiting case $\lambda = 0$ in Eq. (42). Furthermore, the steepest descent direction for the function $\Gamma_s = ||\underline{\Gamma}(\underline{y})||^2 = \underline{\Gamma}(\underline{y})^T\underline{\Gamma}(\underline{y})$ is

$$\underline{\Delta y}_{SD} = - KA^T \underline{\Gamma}(\underline{y}) \tag{44}$$

where K is a positive constant. This is approached by Eq. (42) as $\lambda \to \infty$. Marquardt (See Ref. 9) shows that (a) $||\underline{\Delta y}(\lambda)||^2$ is a continuously decreasing function of λ such that, as $\lambda \to \infty$, $||\underline{\Delta y}(\lambda)||^2 \to 0$ and (b) the angle given by

$$\gamma = \cos^{-1}\left(\frac{\underline{\Delta y}^T \underline{\Delta y}_{SD}}{||\underline{\Delta y}|| \; ||\underline{\Delta y}_{SD}||}\right)$$

is a continuous monotone decreasing function of λ such that, as $\lambda \to \infty$, $\gamma \to 0$. It follows that, since $\underline{\Delta y}_{SD}$ is independent of λ, the vector $\underline{\Delta y}$ rotates toward $\underline{\Delta y}_{SD}$ as $\lambda \to \infty$. In constructing the algorithm, the strategy for adjusting the parameter λ is as follows:

(1) At the k^{th} iteration, $\lambda^{(k)}$ must be chosen such that $\Gamma_s(\underline{y}^{(k+1)}) < \Gamma_s(\underline{y}^{(k)})$. This can always be done in principle if the steepest descent direction is defined and is non-zero. However, this may necessitate choosing a large value of $\lambda^{(k)}$.

(2) $\lambda^{(k)}$ should be reduced toward zero as rapidly as possible when conditions exist which allow convergence with the Newton-Raphson correction vectors. Marquardt defines the following adaptive scheme for carrying this out:

(a) Let $\nu > 1$

(b) Let $\lambda^{(k-1)}$ denote the value of λ from the previous iteration. Initially let $\lambda^{(0)} = 10^{-2}$, say.

(c) Compute $\Gamma_s(\underline{y}^{(k)})\big|_{\lambda^{(k-1)}/\nu}$ and $\Gamma_s(\underline{y}^{(k)})\big|_{\lambda^{(k-1)}}$ where $\Gamma_s(y^{(i)})\big|_\lambda = \Gamma_s(\underline{y}^{(i-1)} + \Delta\underline{y}^{(i-1)}(\lambda))$ and $\Delta\underline{y}$ is calculated from Eq. (42). The superscripts refer to the iteration number.

(d) Then if $\Gamma_s(y^{(k)})\big|_{\lambda^{(k-1)}/\nu} \leq \Gamma_s(\underline{y}^{(k-1)})$, let $\lambda^{(k)} = \lambda^{(k-1)}/\nu$. If $\Gamma_s(\underline{y}^{(k)})\big|_{\lambda^{(k-1)}/\nu} > \Gamma_s(\underline{y}^{(k-1)})$ and $\Gamma_s(y^{(k)})\big|_{\lambda^{(k-1)}} \leq \Gamma_s(\underline{y}^{(k-1)})$, let $\lambda^{(k)} = \lambda^{(k-1)}$. If $\Gamma_s(\underline{y}^{(k)})\big|_{\lambda^{(k-1)}/\nu} > \Gamma_s(y^{(k-1)})$ and $\Gamma_s(y^{(k)})\big|_{\lambda^{(k-1)}} > \Gamma_s(\underline{y}^{(k-1)})$ increase $\lambda^{(k-1)}$ by successive multiplications of ν until for some smallest ω,

$\Gamma_s(\underline{y}^{(k)})\big|_{\lambda^{(k-1)}/\nu^{\omega}} \leq \Gamma_s(\underline{y}^{(k-1)})$ and let

$\lambda^{(k)} = \lambda^{(k-1)}{}_{\nu}\omega.$

Since gradient methods are scale-dependent, Marquardt elects to scale the parameter space by introducing the transformation matrix $D = \text{diag}\,(A^T A)$. The scaled correction vector corresponding to Eq. (42) then becomes

$$\Delta\underline{y} = -\, D^{-1/2}(D^{-1/2}A^T A D^{-1/2} + \lambda I)^{-1} D^{-1/2} A^T \Gamma(\underline{y}) \qquad (45)$$

and this, in conjunction with the procedure above for manipulating λ, constitutes the complete algorithm.

The principal advantage of Marquardt's method lies in its ability to combine the features of steepest descent which exhibit good starting characteristics from an initial guess and the Newton-Raphson procedure which gives fast terminal convergence in the neighborhood of the solution. The adaptive adjustment of the interpolating parameter λ assures that the procedure will not diverge and a finite reduction of $\Gamma_s = ||\underline{\Gamma}(\underline{y})||^2$ is realized on each iteration.

One of the numerical problems which has been found to occur is a very slow rate of convergence so that a large number of iterations gives only a small reduction of the function Γ_s. This situation occurs when the calculated λ becomes reduced so that the angle between $\Delta\underline{y}$ and $\Delta\underline{y}_{SD}$ approaches 90 deg. Thus very little improvement per iteration is obtained. Furthermore, a matrix inversion and a computation of the function gradient is required for each iteration. This latter is a time-consuming operation for dynamic optimization problems which require integration of differential equations for each evaluation of the function Γ_s. Hence, one desires maximum efficient use from each gradient computed. Nevertheless, Marquardt's method is a powerful optimization procedure which can be used effectively to solve two-point boundary value problems. Its performance compares favorably to most first-order optimization techniques which do not exploit known contour features for a given problem.

IV. DISCUSSION AND RESULTS

The true minimum fuel transfer between two given orbits is the Case III problem in which transversality conditions are derived which provide additional information for determining the optimal departure point from the initial orbit and the best final arrival point. Because of the numerical complexities involved, it is convenient to treat this problem as a sequence of subproblems with the boundary conditions completely or partially specified, i.e., the Case I and Case II problems. This approach has several advantages: (1) computational problems are reduced; (2) physical insight into the geometry of low thrust transfers is provided by the optimal solution to the subproblems; (3) sensitivity of the cost function to non-optimal departure and arrival points is available; and (4) existence of multiple extrema can be demonstrated.

A. THE LIMITING CASE I PROBLEM: PHYSICAL BARRIER

Consider the Case I transfer starting from perigee of the initial orbit and proceeding to a specified endpoint on a given co-apsidal final orbit (see Fig. 3). The Multiple Substitution Polynomial method was used to provide the numerical solution for the minimum fuel, continuous low thrust transfers to various points on the terminal orbit, as specified by the final true anomaly ν_f. Figure 4 shows the time variation of the true anomaly on the optimal trajectory for specified ν_f of 270, 240, 210, and 180 deg. Time is normalized for each transfer trajectory by dividing by the total transfer time required. Thus each trajectory has its own normalization factor, and each is plotted against the same fraction of its total time. The optimal solutions show that the true anomaly is nearly a linear function of time for these low-eccentricity orbits, and thus a minimum time transfer acts to minimize the total change in true anomaly.

The Case I problem specifies the $\Delta\nu = \nu_f - \nu_i$ for the transfer and it is evident that there exists some $\Delta\nu_{min}$ which represents a physical limit of the thrust capability of the vehicle. For a fixed ν_i, no Case I solution exists for $\nu_f < \nu_{f_{min}}$ without a large jump in the cost function caused by a transfer of

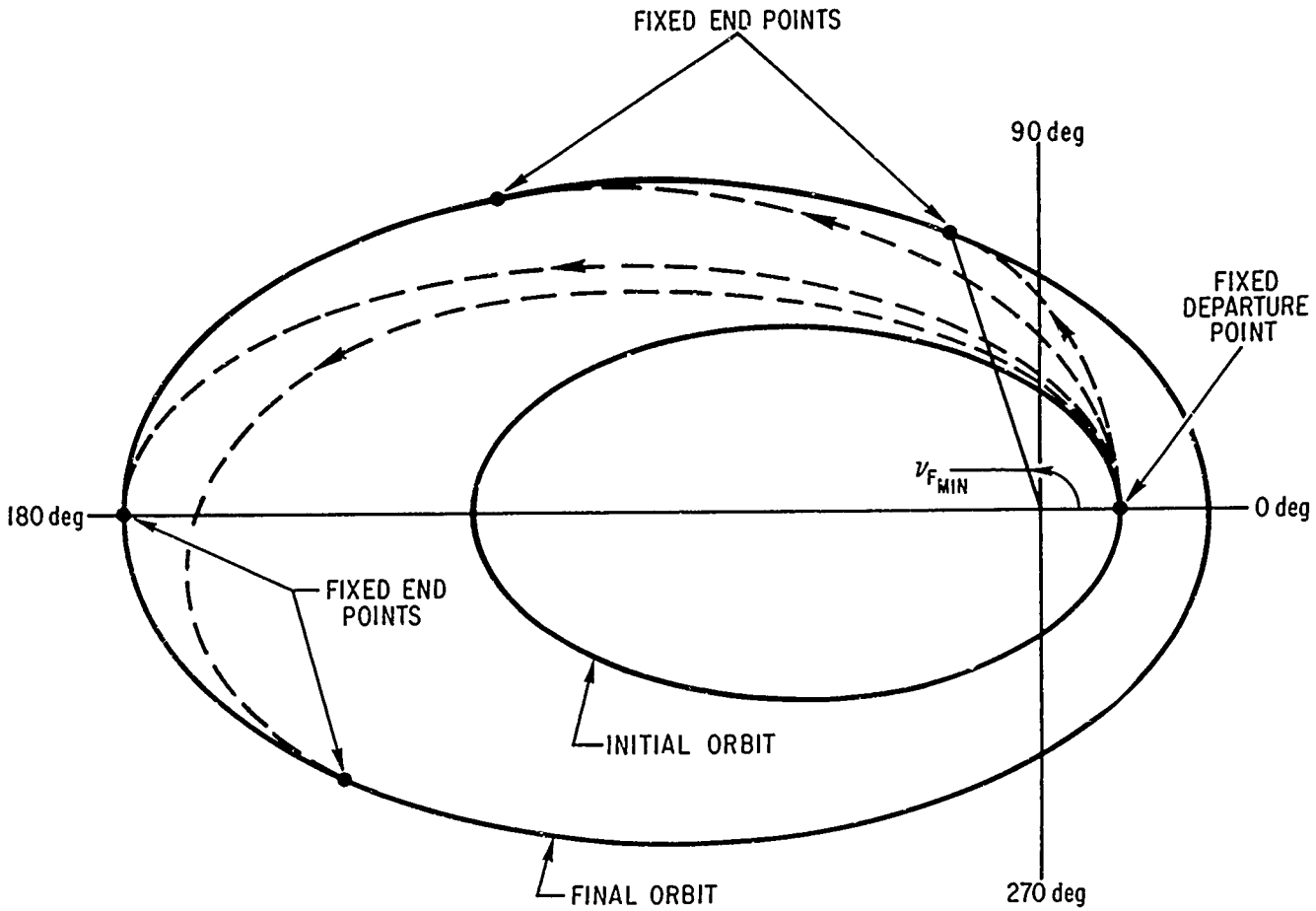

Figure 3. Case I: Fixed Endpoint Transfer Trajectories

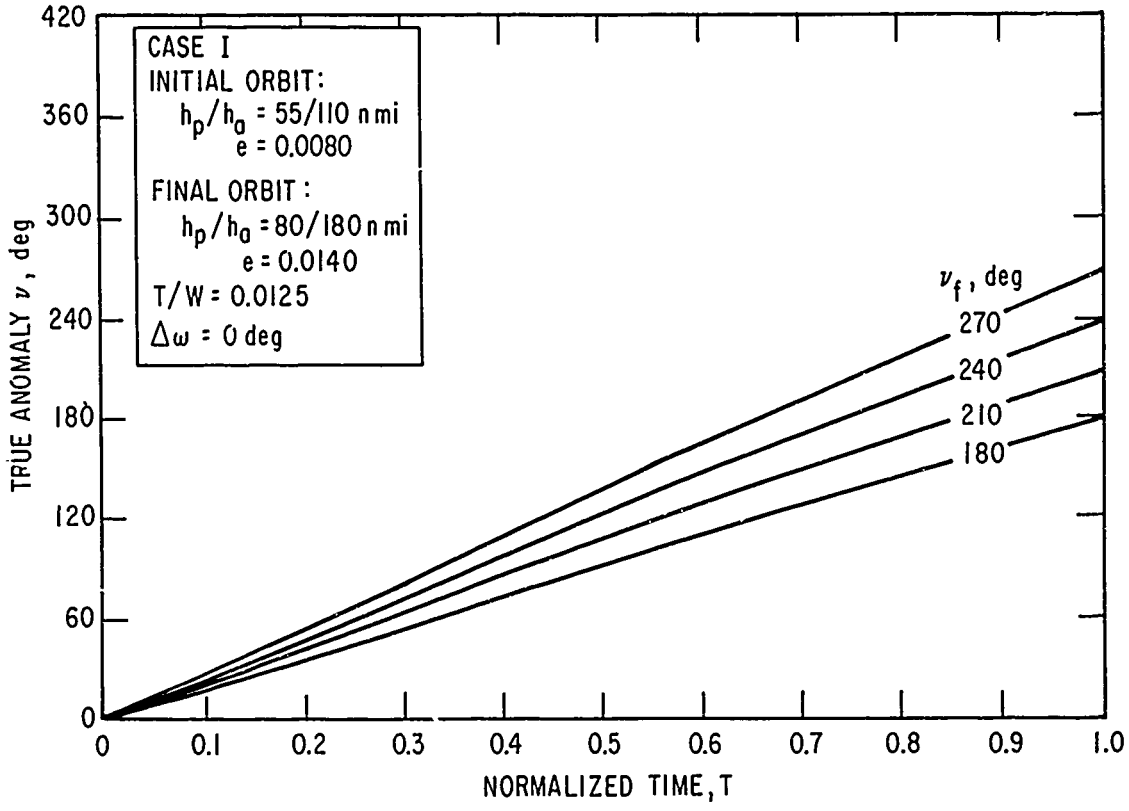

Figure 4. Case I: Time Variation of True Anomaly on Optimal Trajectories

more than one revolution. Thus, the Case II solution represents the limit of the Case I fixed-point transfers as ν_f approaches $\nu_{f\min}$ from above. The $\nu_{f\min}$ is a physical constraint such that no sample points can be evaluated during the iteration process which requires $\nu_f < \nu_{f\min}$.

The sequence of substitute contours for $\underline{\Gamma}(\underline{y})$ generated by the MSP method was found to provide rapid convergence for the specified final points taken over the range 180 deg $\leq \nu_f \leq$ 330 deg, with ν_i fixed at perigee. Approximately 5 iterations were required for complete convergence for a 30 deg change of final true anomaly. However, as ν_f was reduced further, the region of convergence diminished sharply and required a greater number of iterations to produce neighboring solutions for 1 to 5 deg changes in ν_f. The method became completely ineffective for $\nu_f \leq 158$ deg. The actual contours of $\underline{\Gamma}(\underline{y})$ evidently could not be approximated sufficiently accurately because of the effect of the physical border.

Marquardt's method was proved to be useful for extending the solution region for $\nu_f < 158$ deg. This technique acts to minimize the sum of squares of the components of $\underline{\Gamma}$ and, through its adaptive manipulation of the step size parameter, local non-zero minima were sometimes encountered. These had no apparent physical significance and often arrested the convergence process. An increase in numerical sensitivity was observed as the border was approached, and the trajectory integration range partitioning was increased from 100 to 200 steps to preserve numerical accuracy. The rates of change of the optimal initial conditions λ_{10}, λ_{30}, λ_{40} were seen to experience a rapid rate of increase as ν_f was decreased toward the minimum value (See Fig. 5). This caused a reduction in the region of convergence for neighboring solutions as ν_f was varied.

Calculations of the gradient by finite differencing was found to require a careful adjustment of the perturbation parameter δ especially for solutions near ν_f = 155 deg. Figure 6 illustrates the rapid fluctuation in the

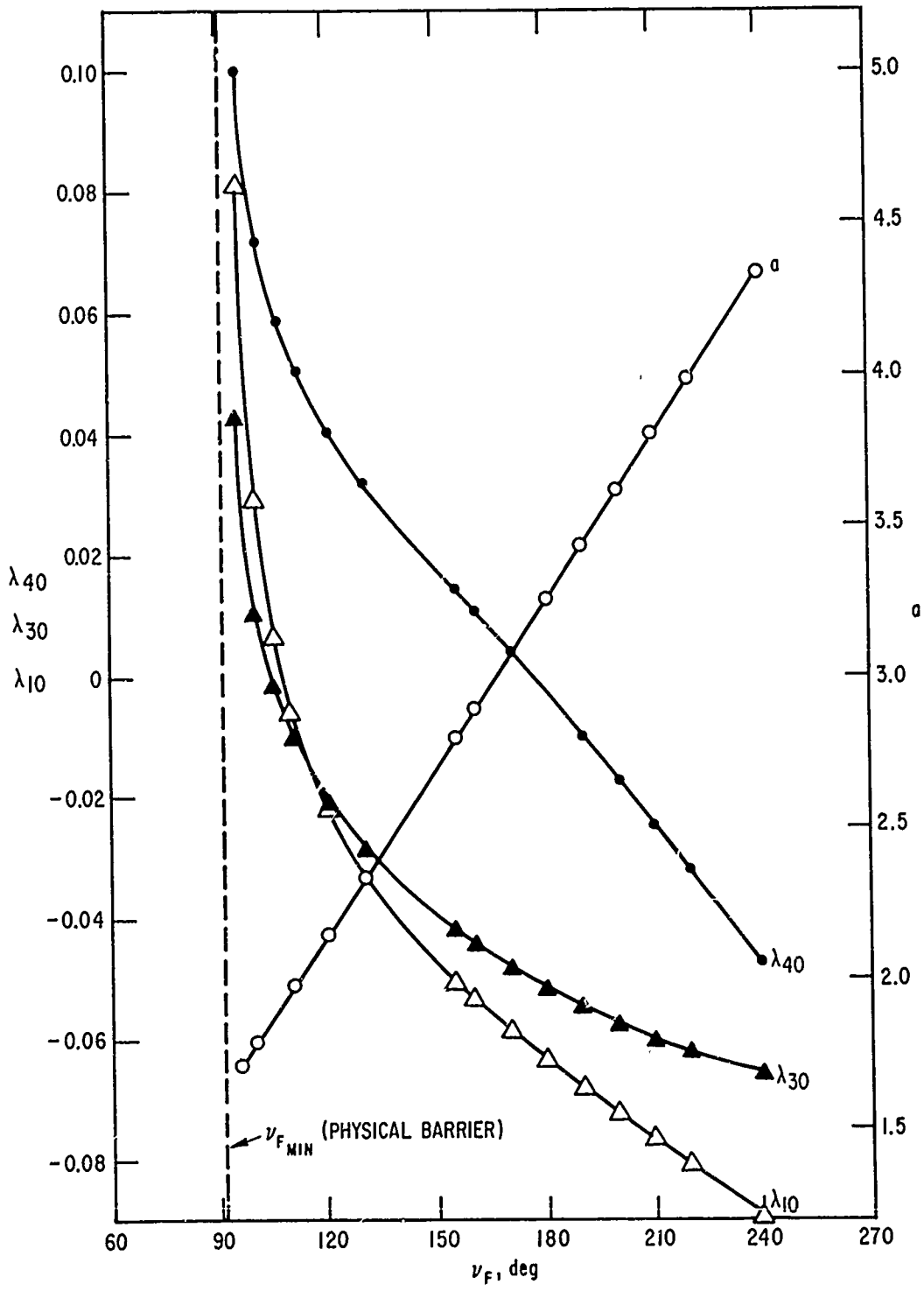

Figure 5. Case I: Optimal Adjoint Initial Conditions versus Specified ν_f

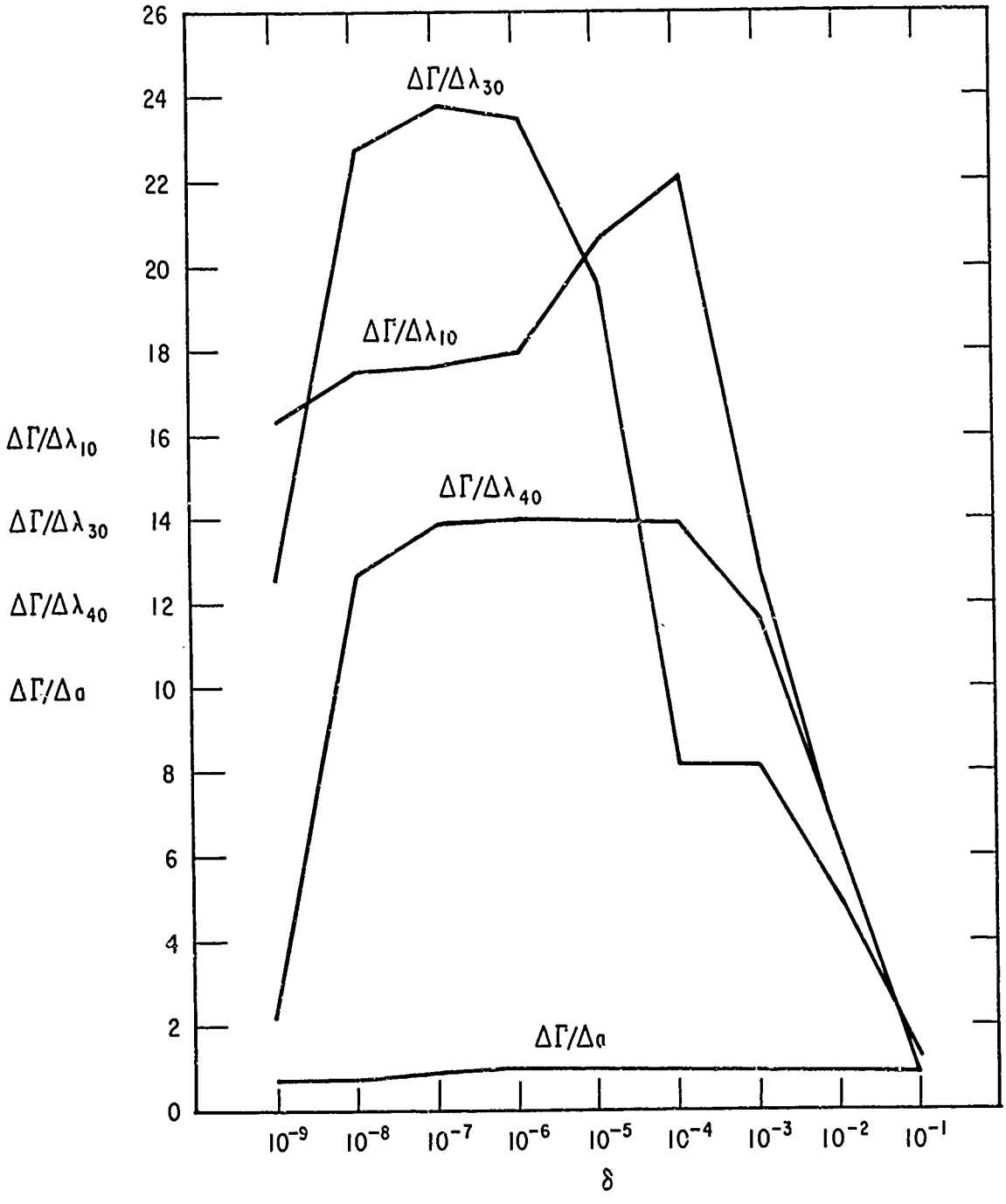

Figure 6. Gradient Calculation: Effect of Differencing Parameter δ for ν_f = 155 deg

approximation to the partial derivative, as computed from

$$\frac{\Delta\Gamma}{\Delta\lambda_{10}} = \frac{\Gamma(\lambda_{10}+\delta,\lambda_{30},\lambda_{40},a) - \Gamma(\lambda_{10},\lambda_{30},\lambda_{40},a)}{\delta}$$

$$\vdots \qquad\qquad \vdots$$

$$\frac{\Delta\Gamma}{\Delta a} = \frac{\Gamma(\lambda_{10},\lambda_{30},\lambda_{40},a+\delta) - \Gamma(\lambda_{10},\lambda_{30},\lambda_{40},a)}{\delta} \tag{46}$$

with δ ranging from 10^{-9} to 10^{-1}. The curves show the finite difference approximations evaluated at the solution for ν_f = 155 deg where, in this case, the scalar Γ is defined by

$$\Gamma = \sum_{i=1}^{4} |\Gamma_i| \tag{47}$$

The significant features to note in Fig. 6 are the restricted range of δ over which the partial derivative approximations remain relatively constant and the rapid falloff of the curves for $\delta \leq 10^{-8}$. This latter point represents the loss of numerical accuracy from integration truncation and roundoff effects, and it fixes the lower limit for δ. Comparison with Fig. 7 shows the relative behavior of the derivative approximations taken about the solution points for ν_f = 240 and 100 deg. Notice that the range over which the curves remain constant extends through $10^{-7} \leq \delta \leq 10^{-4}$, a considerable increase over the restricted range of good approximation $10^{-7} \leq \delta \leq 10^{-6}$ required for the ν_f = 155 deg example. Although no generalizations concerning this phenomenon are evident, it suggests the need for a sensitivity analysis of this kind when using finite difference gradient approximations for dynamic optimization problems.

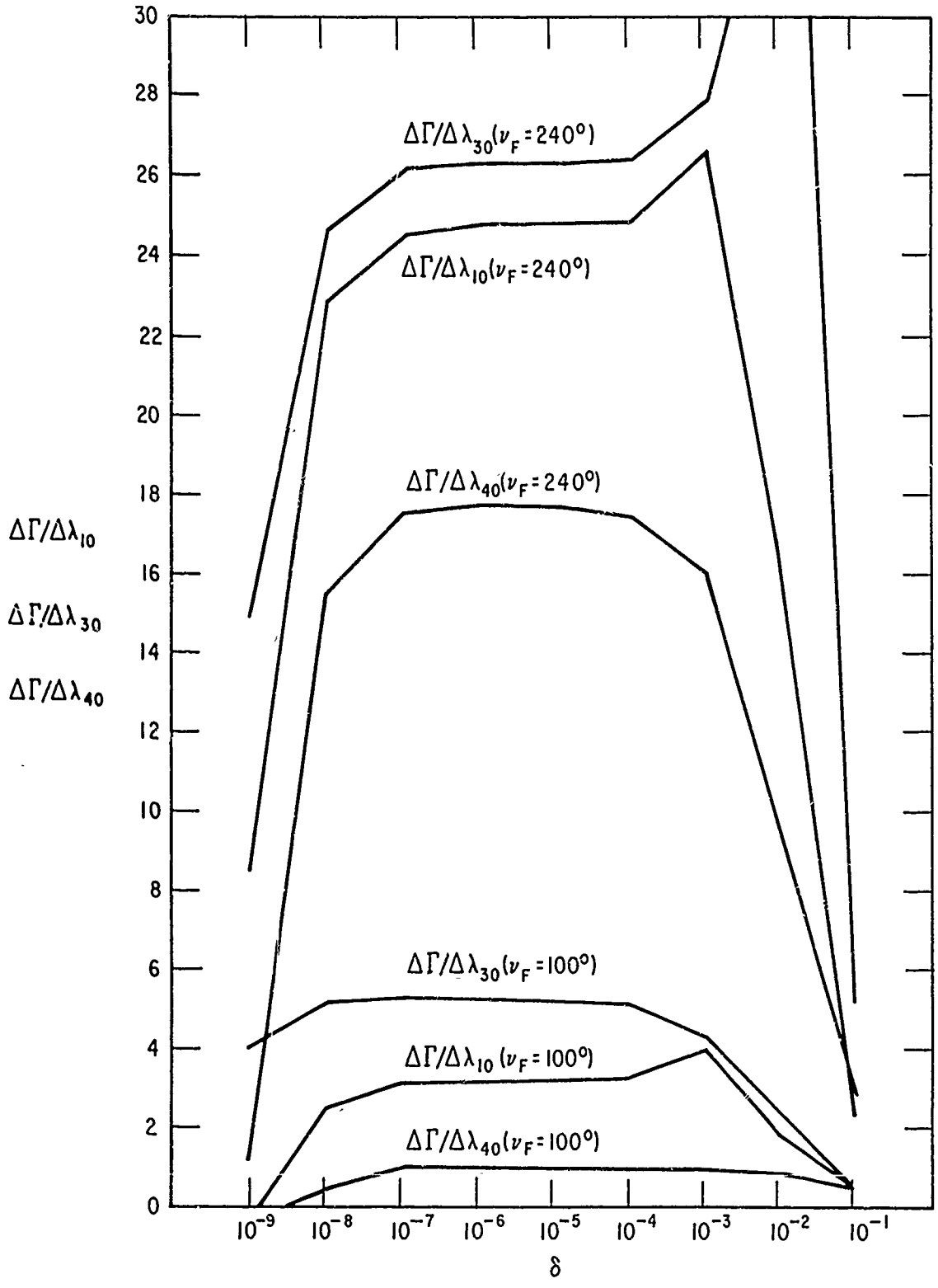

Figure 7. Gradient Calculation: Effect of Differencing Parameter δ for ν_f = 100 deg and 240 deg

Since the absolute value definition is used for Γ [see Eq. (47)], the value of the partial derivatives, as seen in Figs. 6 and 7, evaluated at the solution are not zero but are related to the slopes of the function Γ in the direction of the coordinate axes. As ν_f is taken near the border of the Case I feasible region, these slopes approach zero. The determination of the true limiting point $\nu_{f\,min}$ was made using the Case II problem formulation with the single transversality condition. The optimal Case II transfer from perigee was found to arrive at the final orbit with $\nu_f = \nu_{f\,min} = 90.6$ deg.

B. PARAMETRIC CASE II SOLUTIONS

Marquardt's method was used to generate a sequence of Case II (final endpoint free) solutions, with the specified starting points taken 90 deg apart. Typically, 7 iterations were required for convergence to the new solutions when the initial takeoff point ν_i was changed by a 90-deg interval. Figure 8 shows the optimal transfer trajectories given as a polar plot of altitude versus true anomaly. The arrows indicate the thrust direction and the cross lines mark the point at which the thrust changes sign. If the optimal transfer times (and equivalently fuel expenditure) are plotted as a function of the specified initial true anomaly, the curve of Fig. 9 results. This shows that there is a unique minimum-fuel transfer possible between these given co-apsidal ellipses and furthermore indicates the magnitude of the fuel penalty of initiating the orbit transfer at other than the optimal point. The true minimum was determined by solving the Case III problem with the two transversality conditions, and this gave $\nu_i = 319$ deg as the best departure angle. The optimal transfer trajectory lies in the mutual perigee region and is indicated in Fig. 8. The sequence of Case II solutions served to isolate the proper region for the Case III transfer and provided sufficiently close initial adjoint conditions so that the five-dimensional optimization program gave rapid convergence. The Case I and II problems required only a four-dimensional search as formulated.

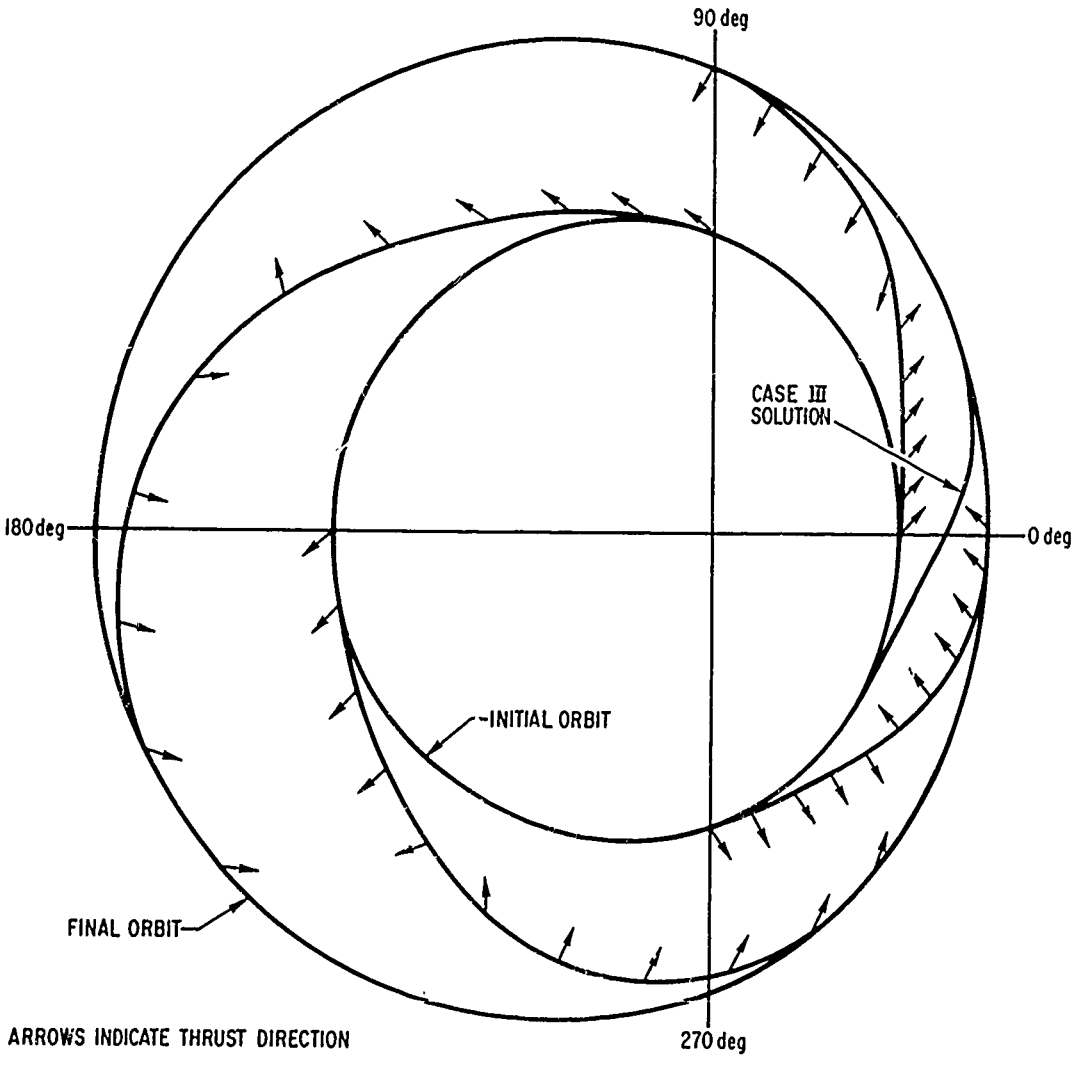

Figure 8. Case II: Polar Plot of Altitude versus True Anomaly for Departure Angles Spread 90 deg Apart

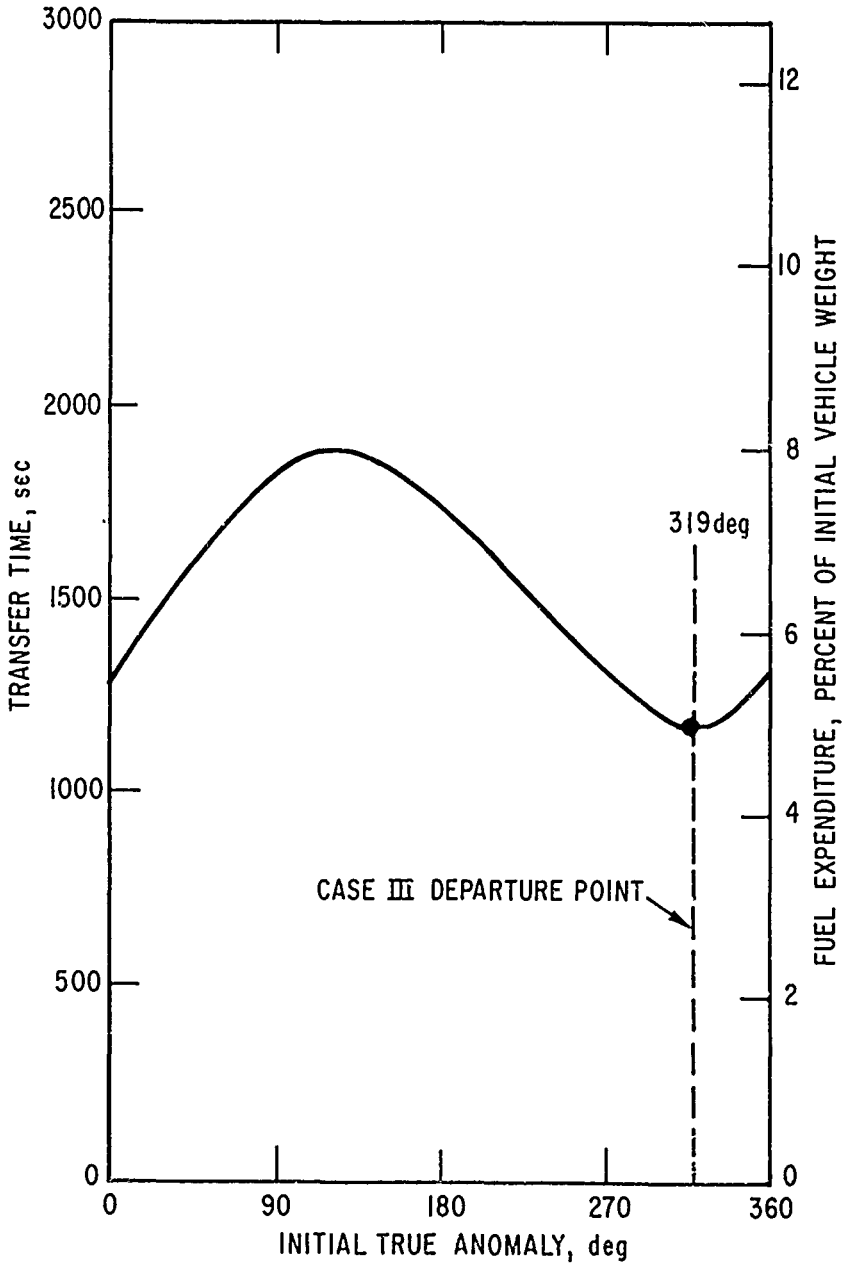

Figure 9. Case II: Transfer Time and Fuel Expenditure versus Initial True Anomaly

C. AXIAL ROTATIONS AND THE MULTIPLE CASE III SOLUTIONS

An example of optimal low-thrust transfer between intersecti g orbits was studied, using the same orbits employed previously but rotated with respect to each other by $\Delta\omega$ = 90 deg. The intersection points were found to occur at ν = 84 deg and 155 deg as measured from perigee of the initial ellipse.

Parametric solutions of the Case II problem were conducted, taking selected starting points around the initial orbit. Severe computational problems arose in the neighborhood of the intersection points where very fast rates of change of the optimal adjoint initial conditions were observed. The nature of the computational barriers is seen in Fig. 10. The solutions in the vicinity of ν_i = 130 deg were especially difficult to obtain since the region of convergence from neighboring solutions was quite limited. This problem was surmounted by increasing the numerical integration accuracy; introducing more precise gradient calculations using symmetric differencing; and reversing the direction of the ν_i parameter variation. In the regions outside of the double spike area shown in Fig. 10, an average of five iterations was sufficient for convergence for a 30 deg change in the specified ν_i, using Marquardt's method.

The results of the Case II parametric study for the 90-deg-rotated geometry are displayed in Fig. 11 which is a plot of the non-dimensional transfer time t_f (scaled by a constant factor), shown as a function of specified departure true anomalies. The existence of multiple extrema is clearly displayed by this technique of using parametric studies of the Case II problem. The corresponding optimal adjoint variable initial conditions from Fig. 10 can thus be selected in the proper regions for finding the multiple minima for the Case III problem, in which neither endpoint is specified. This latter problem requires a five-dimensional search procedure, but good starting values are available through the above technique.

Figure 12 shows three stationary solutions for the Case III orbit transfer with $\Delta\omega$ = 90 deg and displayed as a polar altitude plot. The lesser minimum occurs for the transfer trajectory beginning at ν = 62 deg on the initial ellipse;

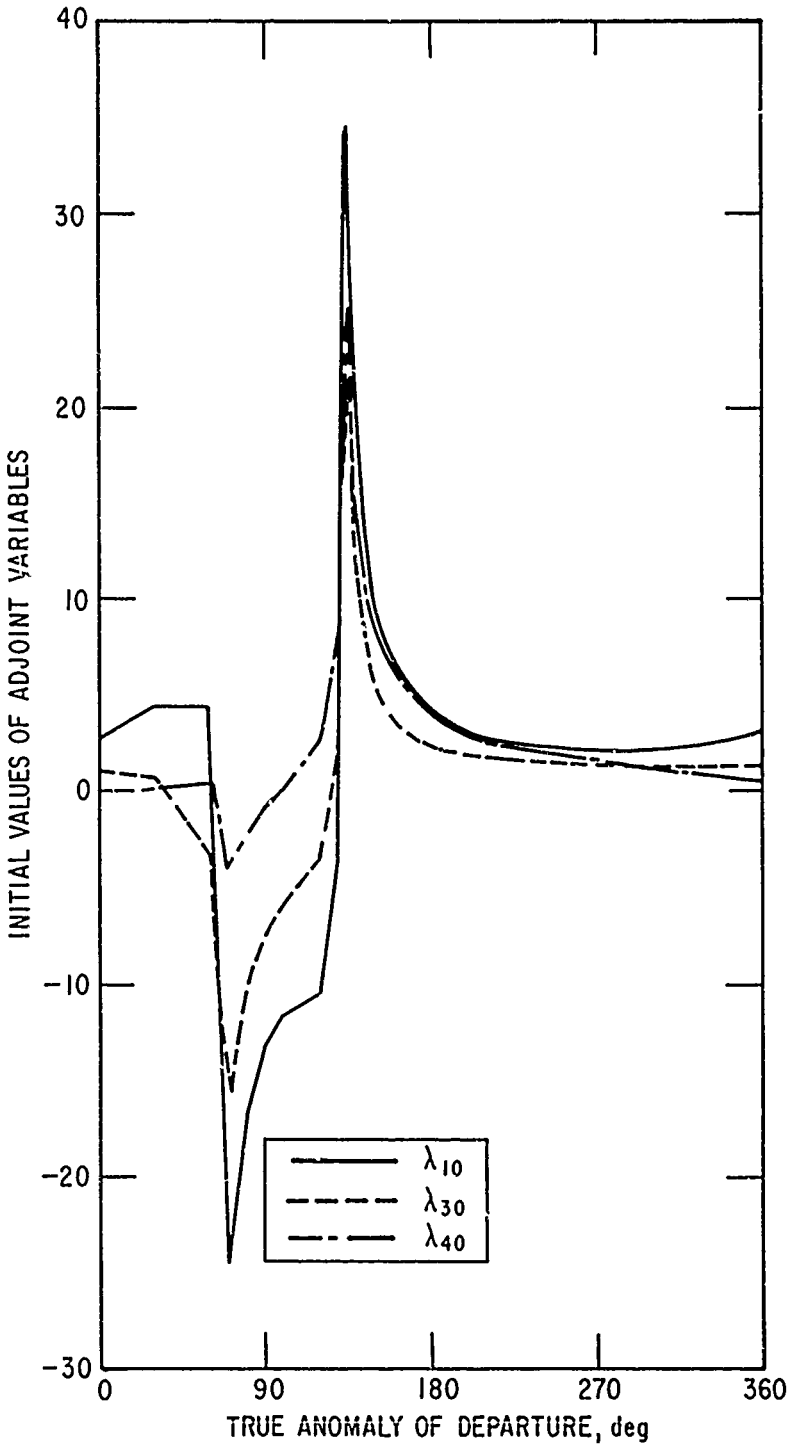

Figure 10. Case II: Initial Values of Adjoint Variables versus True Anomaly of Departure

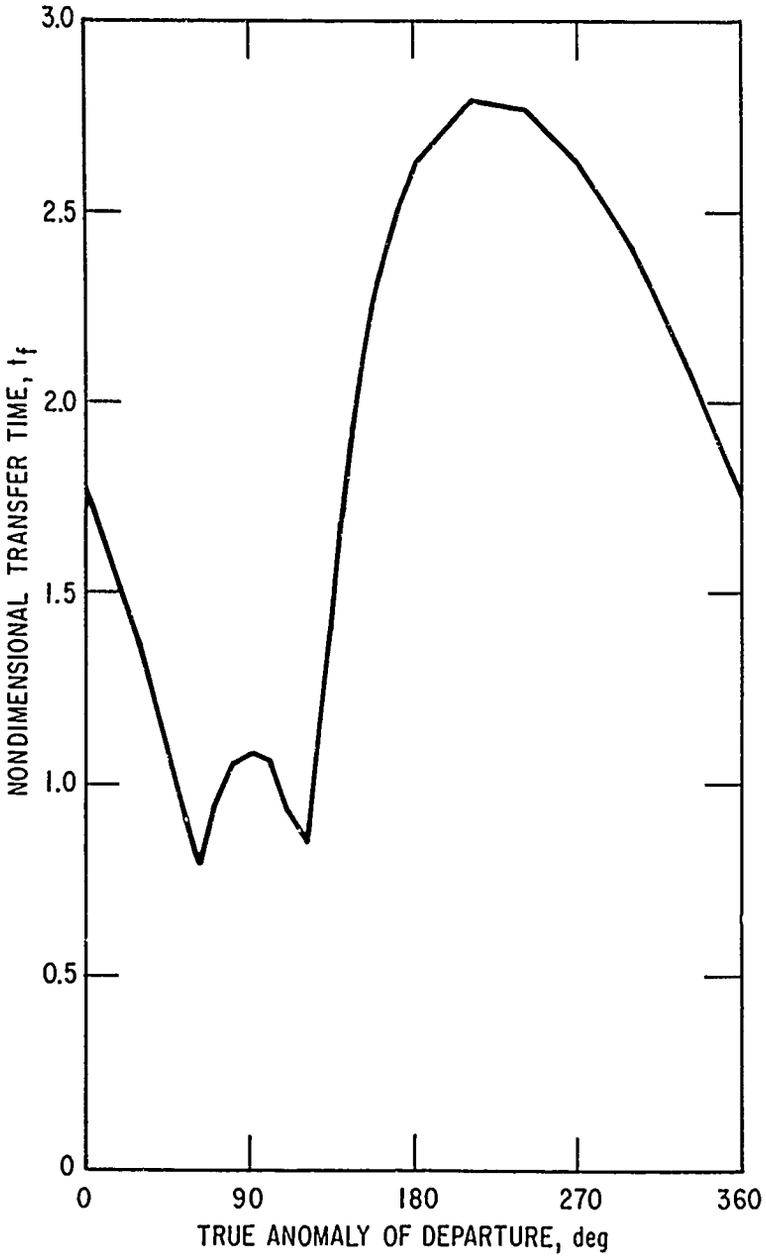

Figure 11. Case II: Nondimensional Transfer Time versus True Anomaly of Departure for $\Delta\omega$ = 90-deg Rotated Orbits

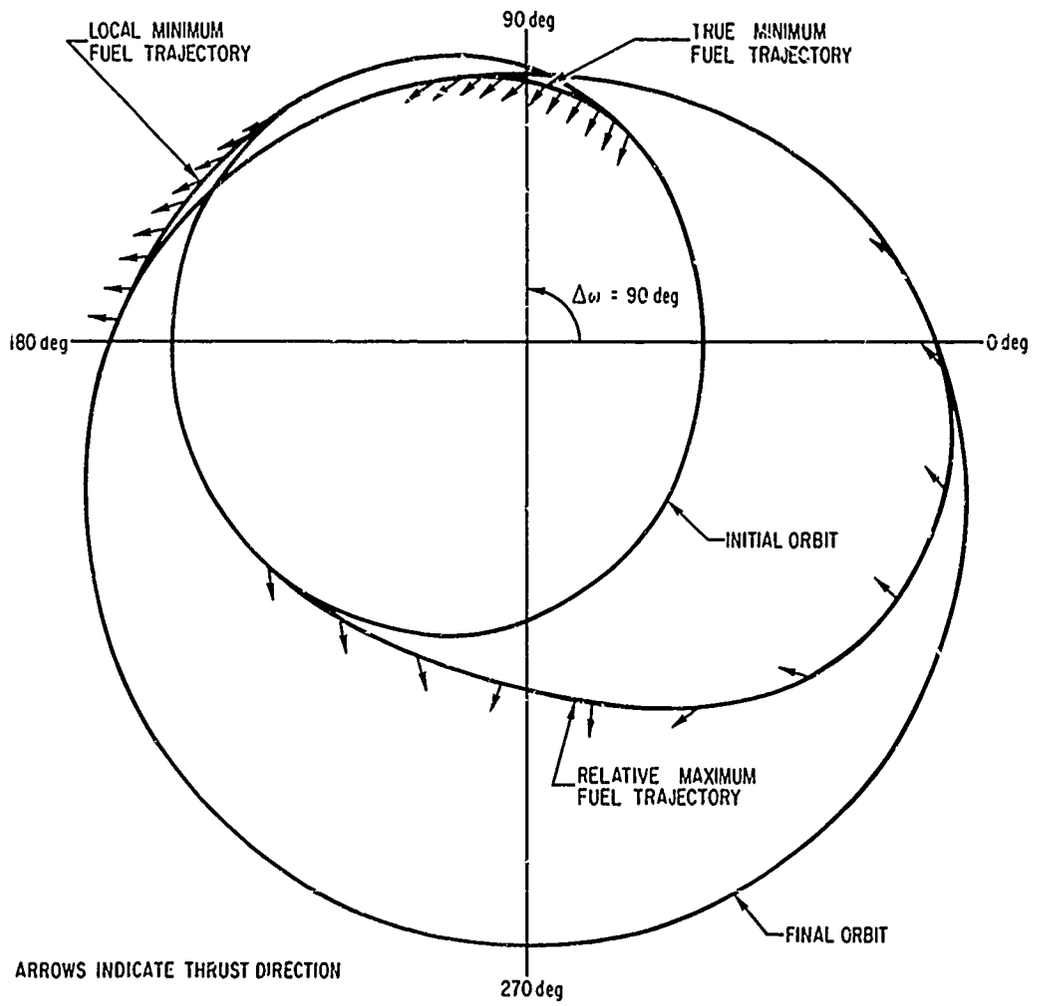

Figure 12. Case III: Polar Plot of Altitude versus Departure Angle for 90-deg Rotated Ellipses

the solution starting at ν_i = 130 deg is a local minimum only. The remaining trajectory represents a relative maximum. A second relative maximal extremum is located between the minimizing solutions but is not shown.

D. PROPERTIES OF THE OPTIMAL LOW THRUST TRAJECTORIES

The optimal Case III continuous low thrust orientation histories for a variety of relative orbit axial rotations $\Delta\omega$ are shown in Fig. 13. The thrust orientation angle ϕ is measured clockwise from the circumferential direction, and each steering history is plotted with respect to the normalized time of its own transfer. A relatively rapid change in thrust direction is seen to occur at the halfway point of the transfer (T = 0.5) for the longer trajectories, as shown by the $\Delta\omega$ = 0 and 30 deg curves. From empirical results, the optimal transfer trajectory appears symmetrical about the point of closest approach of the two orbits. The rate of change of the thrust angle decreases as the transfer distance decreases, as indicated by the $\Delta\omega$ = 60 deg example, although symmetry is preserved. The orbits intersect for $\Delta\omega$ = 84 deg and multiple extrema were found to exist for the $\Delta\omega$ = 90 deg case examined. The optimum thrust orientation history corresponding to the least fuel transfer is shown for the 90 deg rotation case.

The effect of the thrust-to-weight ratio (T/W) on the relative fuel cost and transfer time is shown in Fig. 14. It is seen that, as the thrust capability for a given vehicle is reduced, the transfer maneuver becomes more economical from the fuel cost standpoint but at the expense of an increase in the transfer time. The curves shown were computed for the Case III problem with $\Delta\omega$ = 0 deg.

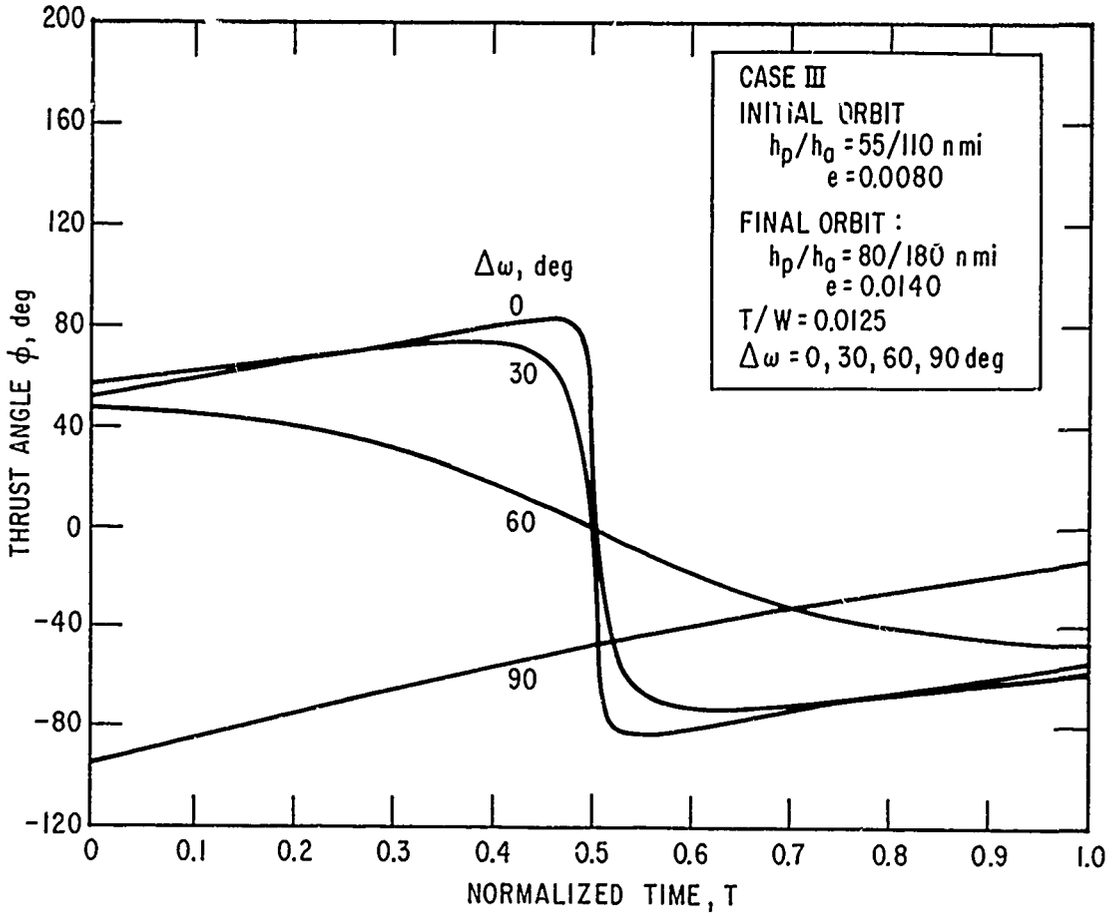

Figure 13. Case III: Optimal Thrust Orientation versus Time for Various Δω

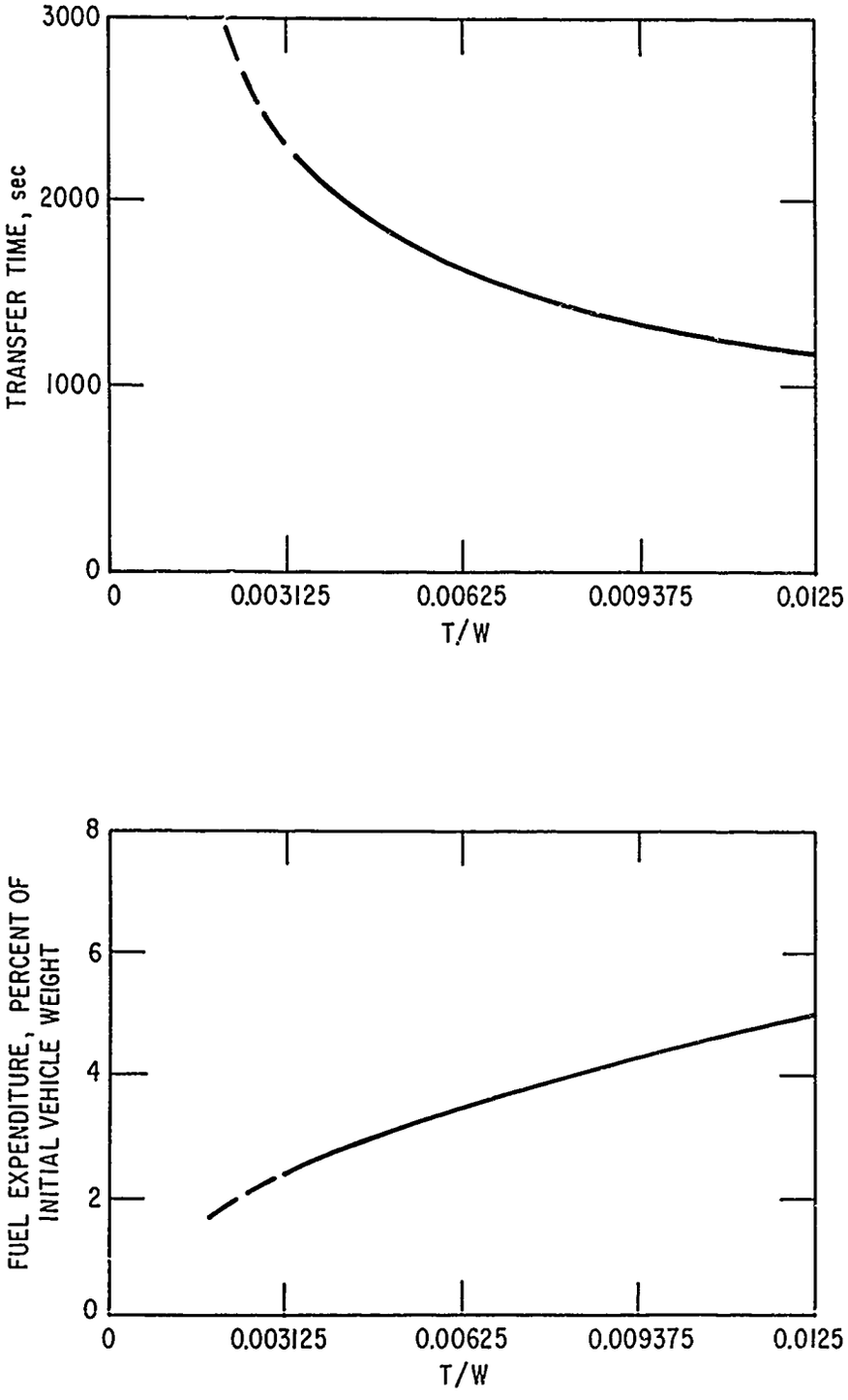

Figure 14. Case III: Transfer Time and Fuel Expenditure versus Thrust-to Weight Ratio

V. SUMMARY AND CONCLUSIONS

Some computational aspects of the optimal continuous low thrust orbit transfer problem have been presented. Numerical solutions were obtained via the method of Multiple Substitution Polynomials and Marquardt's method, indicating their applicability for solving optimal control problems of this type. Formulation of the problem for numerical solution was given, showing how a sequence of subproblems can be used to indicate the existence and location of multiple extrema. Computational problems relating to the breakdown of the numerical technique on restriction of the region of convergence were discussed.

A physical barrier which restricts sample points was found for fixed endpoint transfer problems, and the very rapid variation in the optimal adjoint initial conditions near this region was shown, which accounts for the severe convergence difficulties encountered here.

Parametric studies of the Case II transfers between intersecting orbits were hampered by nearly singular behavior in the $\underline{\lambda}_0$ vs ν_i characteristic which created a computational barrier for isolating the multiple solutions for this problem. This phenomenon was not found for non-intersecting orbits.

Sensitivity problems for calculating the function gradient by finite differencing techniques were encountered, which caused loss of convergence of Marquardt's method in certain transfer regions. The critical adjustment of the differencing parameter δ was demonstrated at several Case II solution points.

The optimal continuous low thrust orbit transfer trajectory for the free endpoints case was empirically found to be symmetrically located with respect to the point of closest approach of the two orbits. A rapid thrust direction reversal was seen to occur at a time equal to approximately one half of the ultimate transfer time when the orbits were nearly co-apsidal. This corresponds to the longer duration optimal transfer maneuvers among the cases studied and the form of this solution is in agreement, for example, with the continuous low thrust Earth-to-Mars rendezvous results reported by Melbourne and Sauer (Ref. 4) and Zimmerman et al (Ref. 5).

From a sequence of Case III solutions with various T/W ratios, it is shown that a vehicle with a larger T/W capability requires more fuel expenditure in transferring between two given orbits than does one with a smaller T/W. The total time for the transfer maneuver constitutes the major tradeoff.

REFERENCES

1. C.R. Faulders, "Minimum-Time Steering Programs for Orbital Transfer with Low Thrust Rockets," Astronaut. Acta 7, 35-49 (1961).

2. S.A. Jurovics, "Orbital Transfer by Optimum Thrust," NASA CR-71027, February 1964.

3. G.A. McCue, "Quasilinearization Determination of Optimum Finite-Thrust Orbital Transfers," AIAA J. 5, 755-763 (1967).

4. W.G. Melbourne and C.G. Sauer, Jr., "Optimum Thrust Programs for Power-Limited Propulsion Systems," JPL Technical Report No. 32-118, June 15, 1961.

5. A.V. Zimmerman, J.S. MacKay, and L.G. Rossa, "Optimum Low Acceleration Trajectories for Interplanetary Transfers," NASA TN D-1456, January 1963.

6. F.T. Smith, "The Application of Dynamic Programming to Orbit Transfer Processes," U.S. Dept. of Commerce Office of Technical Services Report AD-604885, August 1964.

7. R.F. Jaggers, "Polynomial Substitution Formulas and Applications for Solving Boundary-Value and Optimization Problems," paper presented at Intern. Astronaut. Congr., 16th, Athens, Greece, September 16, 1965.

8. J.L. Starr, "Computation of Optimal Control: Solution of the Multi-point Boundary Value Problem," Ph.D. Dissertation, Dept. of Engineering, University of California, Los Angeles, Calif., June 1968.

9. D.W. Marquardt, "An Algorithm for Least-Squares Estimation of Nonlinear Parameters," J. Soc. Ind. Appl. Math. 2, 431-441 (1963).

UNCLASSIFIED

Security Classification

DOCUMENT CONTROL DATA - R&D

(Security classification of title, body of abstract and indexing annotation must be entered when the overall report is classified)

1 ORIGINATING ACTIVITY (Corporate author) Aerospace Corporation El Segundo, California	2a REPORT SECURITY CLASSIFICATION UNCLASSIFIED 2b GROUP

3 REPORT TITLE

SOME COMPUTATIONAL ASPECTS OF THE MINIMUM FUEL CONTINUOUS LOW THRUST ORBIT TRANSFER PROBLEM

4. DESCRIPTIVE NOTES (Type of report and inclusive dates)

5 AUTHOR(S) (Last name, first name, initial)

Starr, James L.
Sugar, Ronald D.

6. REPORT DATE	7a. TOTAL NO. OF PAGES	7b NO. OF REFS
69 AUG Ø4	54	9

8a CONTRACT OR GRANT NO. F04701-68-C-0200, F04701-69-C-0066 b. PROJECT NO c d.	9a. ORIGINATOR'S REPORT NUMBER(S) TR-0066(5306)-3 9b. OTHER REPORT NO(S) (Any other numbers that may be assigned this report) SAMSO-TR-69-283

10 AVAILABILITY/LIMITATION NOTICES

This document has been approved for public release and sale; its distribution is unlimited.

11 SUPPLEMENTARY NOTES	12. SPONSORING MILITARY ACTIVITY
	Space and Missile Systems Organization Air Force Systems Command Los Angeles, California

13. ABSTRACT

The purpose of this paper is to examine the computational aspects of the minimum fuel continuous low thrust orbit transfer problem and to display characteristic numerical features introduced by various physical constraints. Minimum-fuel orbit transfer by low thrust is typical of many problems in optimal control which result in a two point boundary value problem which must be solved by some iterative numerical procedure. Two techniques, Multiple Substitution Polynominals (MSP) and Marquardt's method, are shown to be applicable to this task, and a detailed analysis is made of the behavior of these methods in the context of the low thrust problem. A variety of subproblems is considered with parametric variation of endpoints, thrust-to-weight ratio, and orbit axial orientation. A physical barrier is found which restricts sample points in certain limiting case fixed endpoint transfers. The existence of multiple stationary solutions is shown for the case of intersecting orbits, and the nearly singular behavior in that region is investigated. Numerical results for several transfers are found to compare with similar results reported elsewhere.

DD FORM 1473 (FACSIMILE)

UNCLASSIFIED

Security Classification

14. KEY WORDS

Optimal control
Orbit transfer
Continuous low thrust
Computational techniques
Multiple substitution polynomials
Marquardt's algorithm
Optimization
Calculus of variations
Two-point boundary value problem
Multiple extrema

Abstract (Continued)